Supporting Information

Diphosphazane-monoxide and Phosphine-sulfonate Palladium Catalyzed Ethylene Copolymerization with Polar Monomers: A Computational Study

Jiajie Sun,[a,†] Min Chen,[b,†] Gen Luo,[a] Changle Chen,[b,*] Yi Luo [a,*]

[a]State Key Laboratory of Fine Chemicals, School of Chemical Engineering, Dalian University of Technology, Dalian 116024, China.

[b]Hefei National Laboratory for Physical Sciences at the Microscale, CAS Key Laboratory of Soft Matter Chemistry, iChEM (Collaborative Innovation Center of Chemistry for Energy Materials), Department of Polymer Science and Engineering, University of Science and Technology of China, Hefei 230026, China

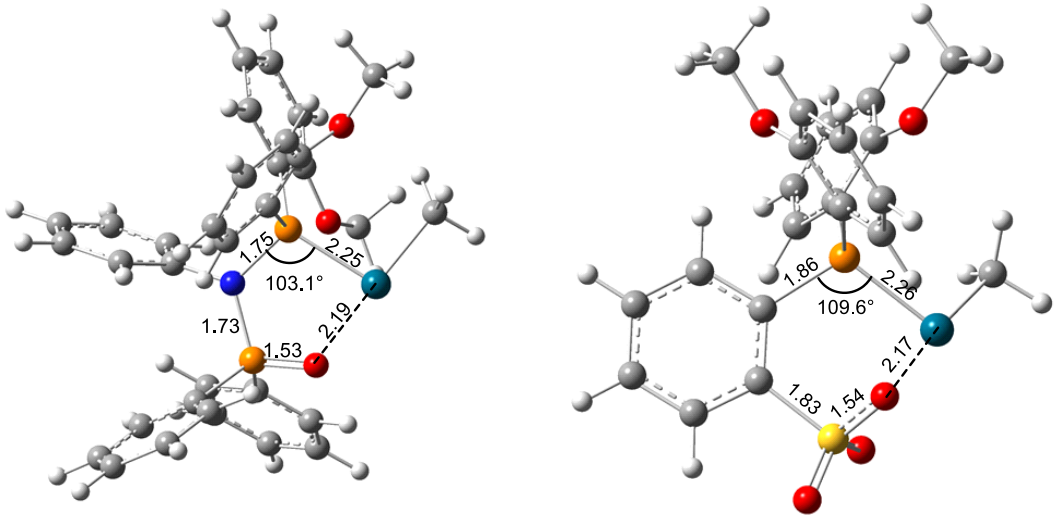

(a) catalyst **A** (b) catalyst **B**

Figure S1. The optimized structures of catalysts **A** and **B** (distances in Å and angles in°).

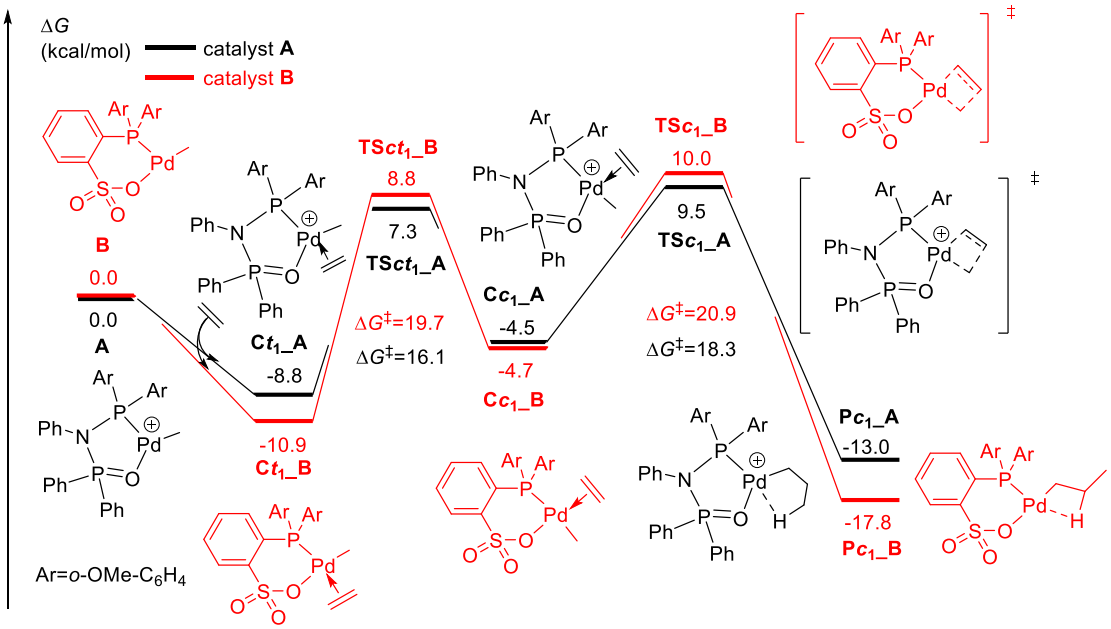

Figure S2. Calculated energy profiles for **A** and **B** mediated insertion of the first monomer ethylene. Free energies are relative to the energy sum of corresponding catalyst and monomer.

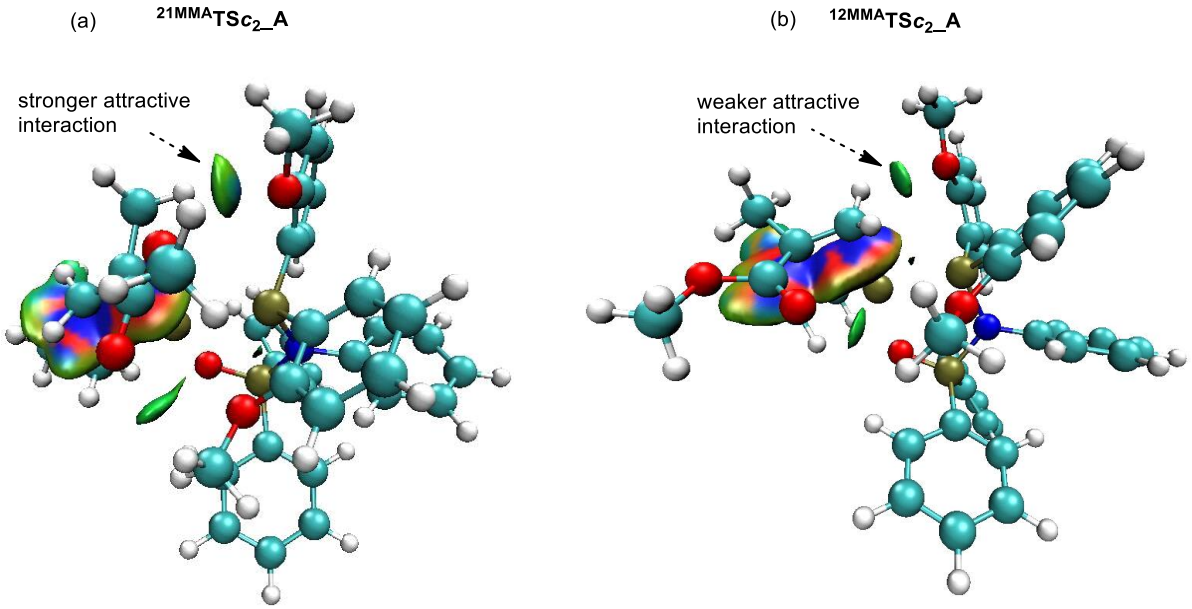

Figure S3. Noncovalent interaction (NCI) analysis for (a) ^{21MMA}**TS***c*$_2$**_A** and (b) ^{12MMA}**TS***c*$_2$**_A**.

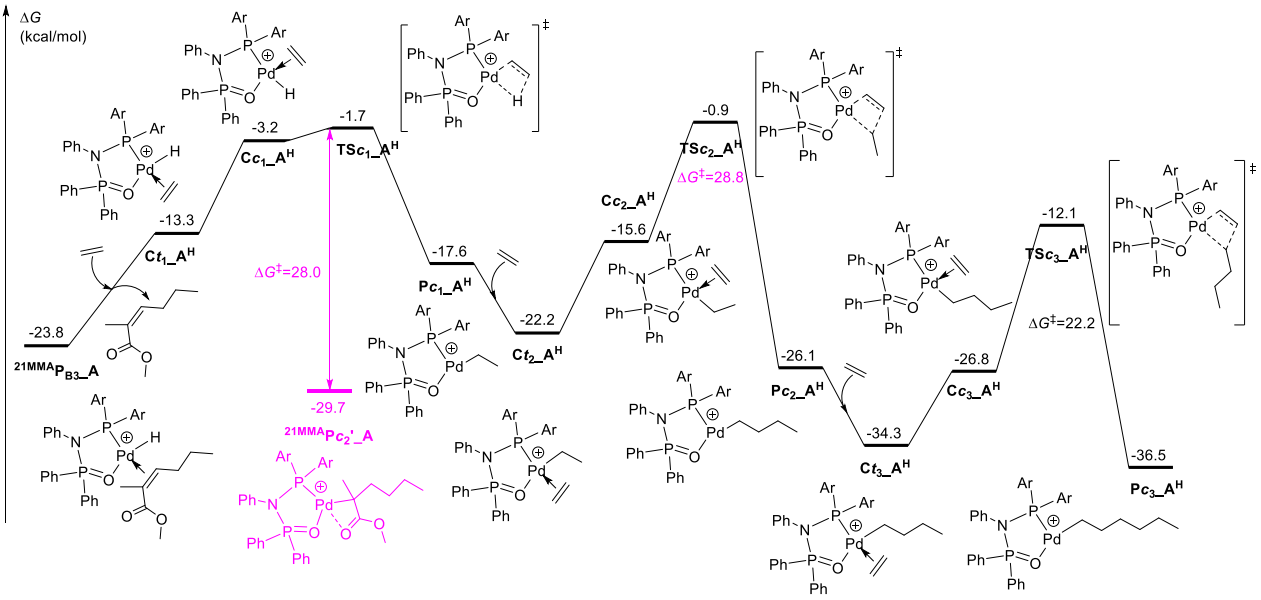

Figure S4. The energy profile for **A** mediated successive ethylene insertion after *β*-H elimination. The overall energy barriers for **TSc$_1$_A^H** and **TSc$_2$_A^H** are relative to the lowest stationary point **^{21MMA}Pc$_2$'_A** in energy (see Figure 6 in the main text), whereas the energy barrier for **TSc$_3$_A^H** is relative to **Ct$_3$_A^H**, which is lower in energy than **^{21MMA}Pc$_2$'_A**.

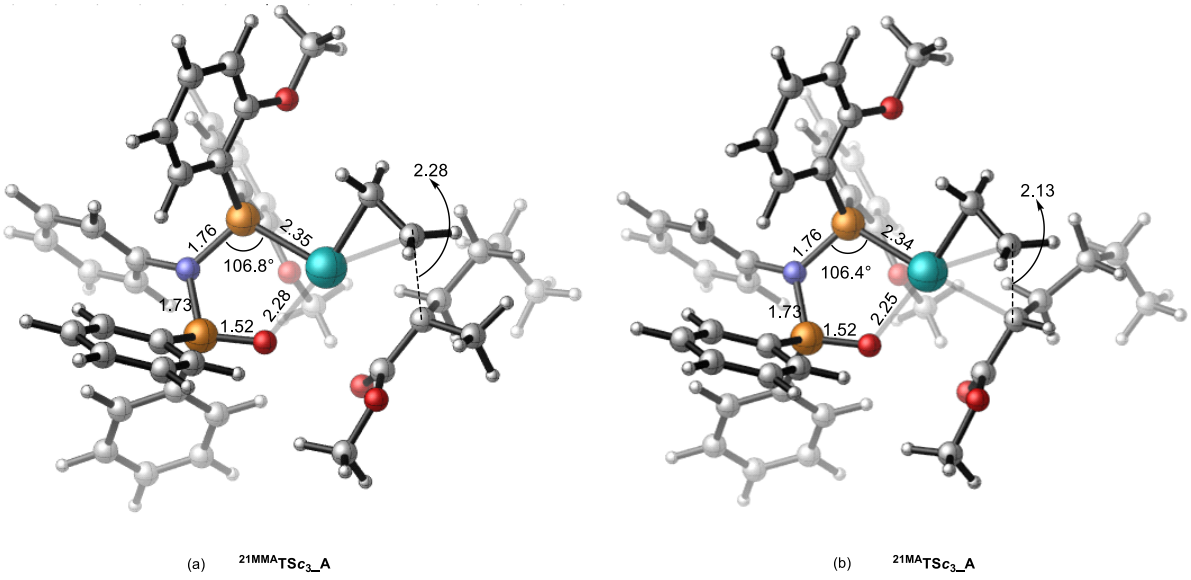

(a) **^{21MMA}TSc$_3$_A** (b) **^{21MA}TSc$_3$_A**

Figure S5. The structures of **^{21MMA}TSc$_3$_A** and **^{21MA}TSc$_3$_A** (distances in Å and angles in°).

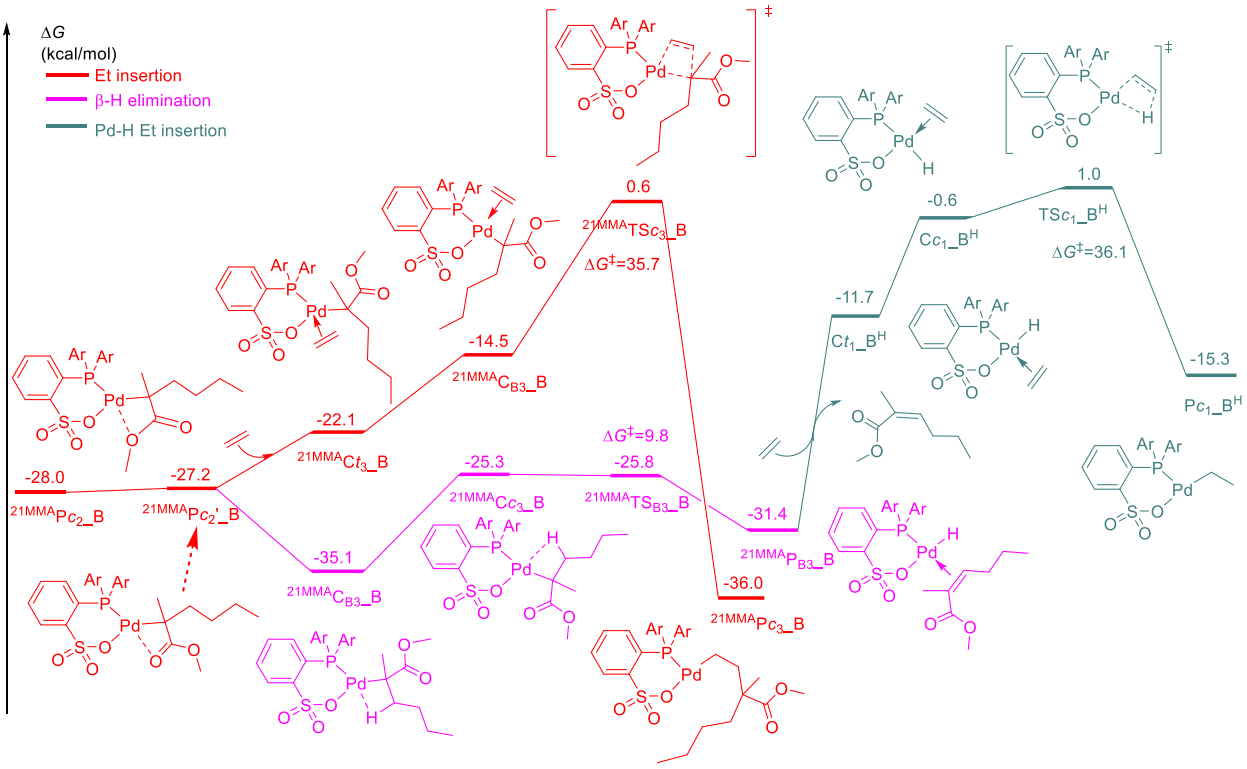

Figure S6. The energy profiles for ^{21MMA}**P*c*$_2$_B** based ethylene insertion and *β*-H elimination as well as the subsequent ethylene insertion into the *β*-H eliminated species. The free energies in solution are relative to **B** and corresponding monomers.

As shown in Figure S6, the intermediate ^{21MMA}**P*c*$_2$_B** with MeO coordination could feasibly isomerize to a more stable *β*-agostic structure ^{21MMA}**C$_{B3}$_B** possibly through ^{21MMA}**P*c*$_2$'_B** with carbonyl coordination. Such a *β*-agostic structure could be hard to achieve *β*-H elimination because of both endergonic character and higher energy barrier for subsequent ethylene insertion into the *β*-H eliminated species (an overall energy barrier of 36.1 kcal/mol). On the other hand, the direct ethylene insertion into ^{21MMA}**P*c*$_2$_B** has an energy barrier of 35.7 kcal/mol relative to ^{21MMA}**C$_{B3}$_B**. As to the MMA 1,2-insertion product ^{12MMA}**P*c*$_2$_B** (shown in Table 2), the subsequent ethylene insertion into ^{12MMA}**P*c*$_2$_B** also computationally suffered from high energy barrier (31.0 kcal/mol) and was therefore unlikely to occur. This intermediate doesn't undergo *β*-H elimination due to the absence of *β*-H atom. These results suggest that MMA could not be incorporated into the polyethylene chain and provide better understanding for the nonoccurrence of copolymerization of MMA and ethylene in **B** catalyst system.

(a)

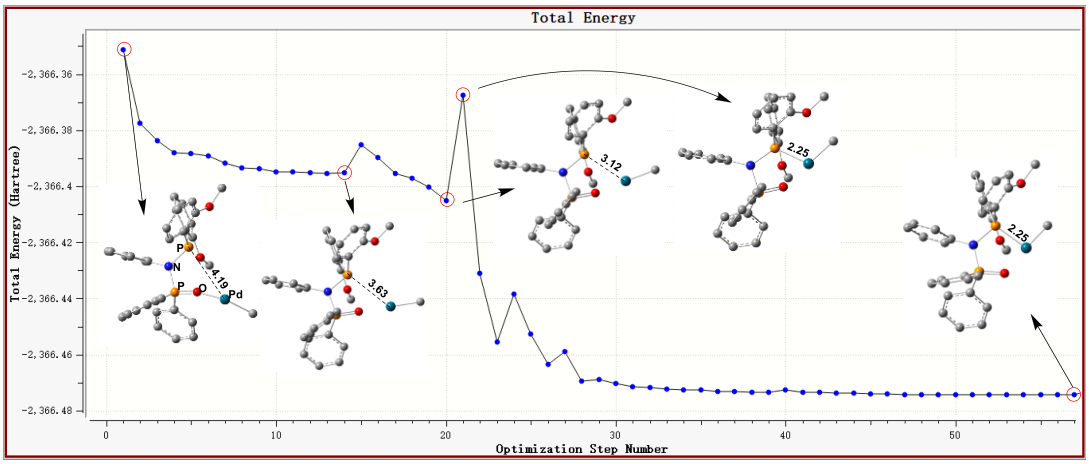

(b)

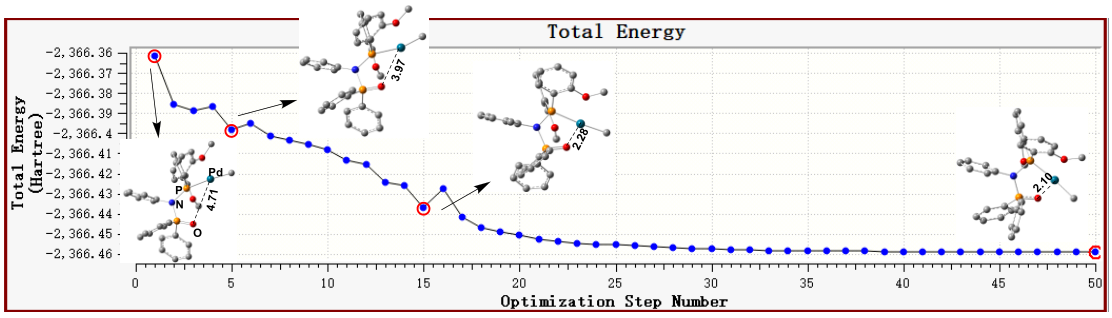

Figure S7. Geometrical optimization processes for (a) an **A**-based model with Pd−P bond dissociation and (b) **A**-based species with Pd−O bond dissociation.

As shown in Figure S7a, starting with an **A**-based model with Pd−P bond dissociation (Pd···P distance of 4.19 Å), the geometrical optimization converged to a stable complex showing coordination of P to Pd center (Pd···P distance of 2.25 Å, same as that in catalyst **A**). Similar case was also observed for a model complex with Pd−O bond dissociation (Pd···O distance of 4.71 Å, Figure S7b). These results indicate that the dissociation of Pd−X (X = P, O) bond could be infeasible in catalyst **A**, possibly due to the rigid ligand backbone and electron deficient nature of the Pd center.

The situation of the Pd−X (X = P, O) dissociation was also computationally investigated for catalyst **B**. As shown in Figure S8, the Pd−O bond dissociation seems to be also infeasible as the species with dissociated Pd−O bond was not located (Figure S8b). On the other hand, the Pd−P bond dissociated species was computationally located (Figure S8a), possibly because of the less electronegativity of P atom compared with O atom. However, this species is higher in free energy in solution than **B** by 44.4 kcal/mol.

These results could add better understanding to that such catalysts work under the ordinary polymerization conditions.

(a)

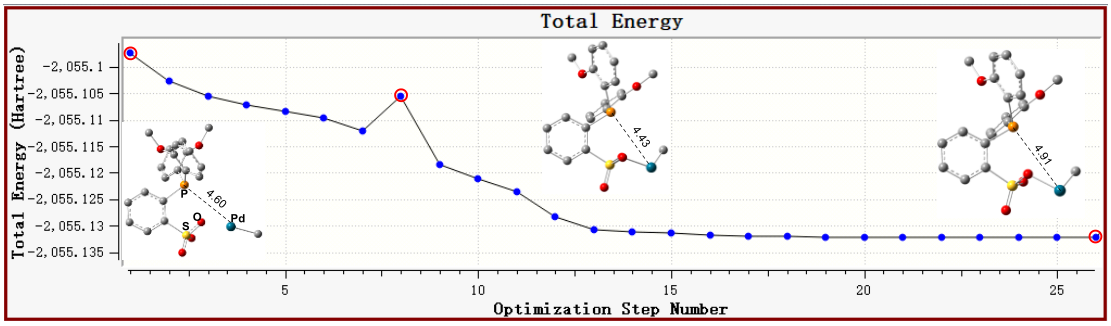

(b)

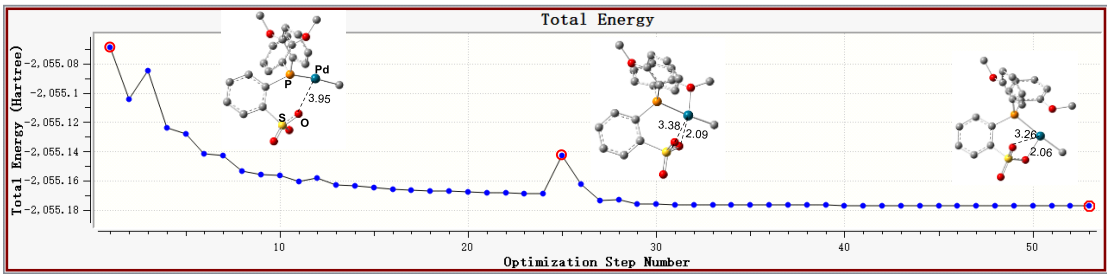

Figure S8. Geometrical optimization processes for (a) a **B**-based model with Pd−P bond dissociation and (b) a **B**-based species with Pd−O bond dissociation.

Table S1. A Comparison of Energy Barriers (kcal/mol) under Different Computational Protocol.

System and Protocol		MMA insertion			MA insertion		
		^{21MMA}**TSc2**	^{12MMA}**TSc2**	barrier difference	^{21MA}**TSc2**	^{12MA}**TSc2**	barrier difference
A	B3LYP	23.6	25.1	1.5	15.9	19.4	3.5
	B3LYP+D3	19.1	24.1	5.0	14.4	19.7	5.3
B	B3LYP	23.9	23.8	-0.1	19.9	21.8	1.9
	B3LYP+D3	21.5	23.5	2	20.5	24..1	3.6

In the case of **A** system, the inclusion of dispersion-corrections in geometry optimizations enlarged the difference in the energy barrier of regioselective insertion (from 1.5 to 5.0 kcal/mol for **MMA**, from 3.5 to 5.3 kcal/mol for **MA**). This indicates that the experimentally observed regioselectivity (favorable 2,1-insertion)[19] is reproduced better when considering the dispersion-correction in geometrical optimization. However, in the case of **B**-mediated **MMA** insertion, the result derived from B3LYP+D3 indicates favorable 2,1-isnertion, which is not so good compared with the experimental observation that both 2,1- and 1,2-insertion product was obtained.[20] These results suggest that the choice of computational protocol can affect the computed results for the current system significantly.

Table S2. Energy Barriers ($\Delta G^{\neq}$, kcal/mol) at Different Temperatures (298.15 *vs*. 353.15 K).

$\Delta G^{\neq}$	ethylene insertion (the first molecule)		MMA insertion (the second molecule)			
	A	**B**	2,1-insertion in **A** system	1,2-insertion in **A** system	2,1-insertion in **B** system	1,2-insertion in **B** system
298.15K[1)]	18.3	20.9	23.6	25.1	23.9	23.8
353.15K	18.4	21.2	24.5	25.8	24.4	24.1
$\Delta\Delta G^{\neq}$	0.1	0.3	0.9	0.7	0.5	0.3

[1)] For the energy barriers at 298.15K, please refer to Table 1 and Table 2 in the main text.

Table S3. The Calculated Relative Free Energies in Solution (kcal/mol) for Insertion of MA[1)]

Catalyst systems	$\mathbf{P}\boldsymbol{c}_1$	$^{MA}\mathbf{C}\boldsymbol{t}_2$,	$^{21MA}\mathbf{C}\boldsymbol{t}_2$ $^{12MA}\mathbf{C}\boldsymbol{t}_2$	$^{21MA}\mathbf{C}\boldsymbol{c}_2$ $^{12MA}\mathbf{C}\boldsymbol{c}_2$	$^{21MA}\mathbf{TS}\boldsymbol{c}_2$ $^{12MA}\mathbf{TS}\boldsymbol{c}_2$	$^{21MA}\mathbf{P}\boldsymbol{c}_2$ $^{12MA}\mathbf{P}\boldsymbol{c}_2$	$\Delta G_2^{\neq}$ ($^{21MA}\boldsymbol{c}_2$) $\Delta G_2^{\neq}$ ($^{12MA}\boldsymbol{c}_2$)
A	-13.0	-19.8	-17.2	-15.0	-3.9	-27.4	15.9
			-19.0	-13.2	-0.4	-25.6	19.4
B	-17.8	-22.1	-16.7	-12.4	-2.2	-32.8	19.9
			-17.3	-12.0	-0.3	-35.8	21.8

[1)] In the labelling of stationary points, the capital letters **P**, **C**, and **TS** denote the product, coordination complex, and insertion transition state, respectively. The italic lowercase letters ***t*** and ***c*** represent the *trans*- and *cis*-site, respectively. The subscript numbers means the order of monomer. That is, $\mathbf{P}\boldsymbol{c}_1$ denotes the ethylene pre-inserted species; $\mathbf{C}\boldsymbol{t}_2$**'** and $\mathbf{C}\boldsymbol{c}_2$**'** represent the carbonyl oxygen *trans*- and *cis*-site coordinating complexes, respectively; $\mathbf{C}\boldsymbol{t}_2$ and $\mathbf{C}\boldsymbol{c}_2$ denote the C=C double bond *trans*- and *cis*-site coordinating complexes, respectively; $\mathbf{TS}\boldsymbol{t}_2$/$\mathbf{TS}\boldsymbol{c}_2$ and $\mathbf{P}\boldsymbol{t}_2$/$\mathbf{P}\boldsymbol{c}_2$ stand for the corresponding transition states and products, respectively. $\Delta G_2^{\neq}$ represents the insertion free-energy barrier. The energies of the stationary points are relative to the corresponding catalyst and monomer.

Table S4. The Calculated Relative Free Energies in Solution (kcal/mol) for the Insertion of Polar Monomer into Ethylene Pre-Inserted Species[1)]

Catalyst systems[2)]	$\mathbf{P}\boldsymbol{c}_1$	$\mathbf{C}\boldsymbol{t}_2$' $\mathbf{C}\boldsymbol{c}_2$'	$\mathbf{C}\boldsymbol{t}_2$ $\mathbf{C}\boldsymbol{c}_2$	$\mathbf{TS}\boldsymbol{t}_2$ $\mathbf{TS}\boldsymbol{c}_2$	$\mathbf{P}\boldsymbol{t}_2$ $\mathbf{P}\boldsymbol{c}_2$	$\Delta G_2^{\neq}$ (*trans*) $\Delta G_2^{\neq}$ (*cis*)
A-MA	-13.0	-19.8	-17.2	5.1	-15.3	24.9
		-11.4	-15.0	-3.9	-27.4	11.1(15.9)
B-MA	-17.8	-22.1	-16.7	8.0	-31.3	30.1
		-10.2	-12.4	-2.2	-32.8	15.6(19.9)
A-MMA	-13.0	-22.0	-19.3	4.2	-14.6	26.2
		-10.3	-11.8	1.6	-22.2	14.6(23.6)
B-MMA	-17.8	-21.9	-16.1	12.9	-28.8	34.8
		-8.5	-9.3	1.9	-33.0	11.2(23.8)

[1)] In the labelling of stationary points, the capital letters **P**, **C**, and **TS** denote the product, coordination complex, and insertion transition state, respectively. The italic lowercase letters ***t*** and ***c*** represent the

trans- and *cis*-site, respectively. The subscript numbers means the order of monomer. That is, **P*c*$_1$** denotes the ethylene pre-inserted species; **C*t*$_2$'** and **C*c*$_2$'** represent the carbonyl oxygen *trans*- and *cis*-site coordinating complexes, respectively; **C*t*$_2$** and **C*c*$_2$** denote the C=C double bond *trans*- and *cis*-site coordinating complexes, respectively; **TS*t*$_2$**/**TS*c*$_2$** and **P*t*$_2$**/**P*c*$_2$** stand for the corresponding transition states and products, respectively. $\Delta G_2^{\neq}$ represents the insertion free-energy barrier, and the data in parenthesis is the energy barrier relative to the more stable coordination complex (*trans*-site). The energies of the stationary points are relative to the corresponding catalyst and monomer.

[2)] The favorable 2,1-insertion was adopted, except for the **B**-MMA case where the 1,2-insertion manner was considered in view of its thermodynamic priority (Table 2 in the main text).

Table S5. The Calculated Free Energies in CH_2Cl_2 Solution for MMA insertion into Pd−Me bond of B catalyst.

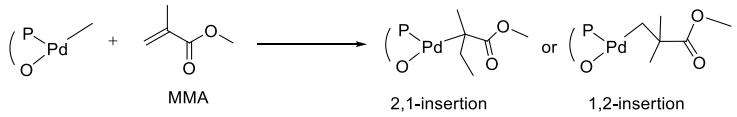

	^{MMA}**C*t*$_2$'_B_Me**	^{12MMA}**TS*c*$_2$_B_Me**	$\Delta G_{12}^{\neq}$	^{21MMA}**TS*c*$_2$_B_Me**	$\Delta G_{21}^{\neq}$
Free energy in solution	-2402.39650 a.u.	-2402.35963 a.u.	23.1 kcal/mol	-2402.35955 a.u.	23.2 kcal/mol

Note: The free energies in CH_2Cl_2 solution include gas-phase free energy correction (353.15 K). The computational method is same as that described in the main text. Since the carbonyl coordination complex is lower in energy than the vinyl coordination complex (Table 2), the energy barriers ($\Delta G_{12}^{\neq}$ for 1,2-insertion TS **^{12MMA}TS*c*$_2$_B_Me** and $\Delta G_{21}^{\neq}$ for 2,1-insertion TS **^{21MMA}TS*c*$_2$_B_Me**) are relative to the carbonyl coordination complex **^{MMA}C*t*$_2$'_B_Me**.

Procedure for the copolymerization of ethylene and methyl acrylate (Reference 39).

In a typical experiment, a 350 mL glass thick-walled pressure vessel was charged with a magnetic stir bar, toluene and the polar monomer (1 M/L, 18 mL in total volume) in a glovebox. The pressure vessel was connected to a high-pressure line and the solution was degassed. The vessel was warmed to 80 °C using an oil bath and allowed to equilibrate for 15 min. The metal complex **A** or **B** (20 μmol) in CH_2Cl_2 (2 mL) was injected into the polymerization system via syringe. With rapid stirring, the reactor was pressurized with ethylene, which was maintained at 8.0 atm. After 6 h, the pressure vessel was vented and the polymer was precipitated in acidified methanol (methanol/HCl = 50/1) and dried at 50 °C for 24 h under vacuum.